



Universiteit  
Leiden  
The Netherlands

## Shot noise from which-path detection in a chiral Majorana interferometer

Beenakker, C.W.J.

### Citation

Beenakker, C. W. J. (2025). Shot noise from which-path detection in a chiral Majorana interferometer. *Physical Review B*, 112(8). doi:10.1103/hgct-3ndj

Version: Publisher's Version

License: [Licensed under Article 25fa Copyright Act/Law \(Amendment Taverne\)](#)

Downloaded from: <https://hdl.handle.net/1887/4282467>

**Note:** To cite this publication please use the final published version (if applicable).

## Shot noise from which-path detection in a chiral Majorana interferometer

C. W. J. Beenakker 

*Instituut-Lorentz, Universiteit Leiden, P.O. Box 9506, 2300 RA Leiden, The Netherlands*



(Received 30 May 2025; revised 30 June 2025; accepted 2 July 2025; published 5 August 2025)

We calculate the full counting statistics of charge transfer in a chiral Majorana interferometer—a setup where a Dirac mode (an electron-hole mode) is split into two Majorana modes that encircle a number of  $h/2e$  vortices in a topological superconductor. Without any coupling to the environment it is known that the low-energy charge transfer is deterministic: an electron is transferred either as an electron or as a hole, dependent on the parity of the vortex number. We show that a stochastic contribution appears if which-path information leaks into the environment, producing the shot noise of random  $2e$  charge transfers with binomial statistics. The Fano factor (dimensionless ratio of shot noise power and conductance) increases without bound as the which-path detection probability tends to unity.

DOI: [10.1103/hgct-3ndj](https://doi.org/10.1103/hgct-3ndj)

**Introduction.** Because a Majorana fermion has a real wave function, only phase shifts  $0$  or  $\pi$  are allowed in a scattering process [1,2]. This restriction is at the basis of the  $\mathbb{Z}_2$  interferometer in a topological superconductor [3–10]: a chiral Dirac mode splits into a pair of chiral Majorana modes, which recombine after having encircled a number  $N_v$  of  $h/2e$  vortices (see Fig. 1). Depending on the  $\mathbb{Z}_2$ -valued parity of  $N_v$ , a low-energy electron (charge  $+e$ ) is transferred through the interferometer either as a  $+e$  electron or as a  $-e$  hole. (In the latter case the missing  $2e$  charge is absorbed by the superconducting condensate.) This charge transfer is noiseless, fully deterministic.

In an electronic Aharonov-Bohm interferometer the oscillatory magnetic field dependence of transport properties is damped by decoherence due to coupling to the environment. The mechanism is which-path detection [11,12]: if the pathway taken by the electron through the interferometer leaves a trace in the environment, no quantum interference of different pathways can occur. Here we wish to examine this effect in the  $\mathbb{Z}_2$  interferometer. We find that which-path detection adds a stochastic contribution to the charge transfer statistics, producing shot noise as a signature of decoherence in Majorana interferometry.

The present study is an application to a topological superconductor of a general method, which I recently developed with Jin-Fu Chen [13]. A chiral interferometer is modeled by a monitored quantum channel [14], in which unitary propagation alternates with weak measurements of the occupation number. It was shown in Ref. [13] for a quantum Hall interferometer that the generalized Levitov-Lesovik formula [15,16] following from this quantum-information-based approach preserves the binomial form of the charge transfer probability expected for Fermi statistics [17], thereby removing a shortcoming of the dephasing-probe model of decoherence [18–22].

Here we find as well that the full counting statistics is binomial, with random charge transfers of size  $2e$  rather than  $e$ , associated with the presence of a superconducting condensate. The Fano factor  $F$ , the dimensionless ratio of shot

noise power and conductance [17], of the Majorana interferometer is anomalous, very different from the quantum Hall effect: we find that  $F$  increases monotonically from zero to arbitrarily large values as the which-path detection becomes more and more effective.

**Full counting statistics of the  $\mathbb{Z}_2$  interferometer.** The central object for the full counting statistics is the cumulant generating function  $C(\xi)$  of the number of electron charges transferred in a time  $t_{\text{counting}}$ , in the limit  $t_{\text{counting}} \rightarrow \infty$ . We assume elastic scattering, so we can consider separately the contribution of each energy  $E$  to the cumulants,

$$C(\xi) = \sum_E \ln F(\xi, E), \quad F(\xi, E) = \langle e^{\xi Q(E)} \rangle, \quad (2.1)$$

with  $F(\xi, E)$  the moment generating function of the charge  $Q(E)$  transferred at energy  $E$ . Charge is measured in units of the electron charge  $e$  and energy is discretized in units of  $\delta E = h/t_{\text{counting}}$ . At zero temperature and a bias voltage  $V > 0$ , energies in the range  $0 < E < eV$  contribute. We will now focus on a single  $E > 0$ , and then at the end sum over all energies.

Following the general method of Ref. [13], we consider a weak measurement of the occupancy of the Majorana mode in each of the arms of the interferometer: mode number  $n = 1$  in the upper arm, mode number  $n = 2$  in the lower arm, see Fig. 2. The measurement of mode  $n$  interpolates with a weight factor  $\varepsilon_n$  between the identity  $\hat{I}$  and a projection onto a filled ( $\hat{P}_{+,n}$ ) or empty ( $\hat{P}_{-,n}$ ) mode:

$$\begin{aligned} \hat{P}_{+,n} &= \delta_n \hat{I} + \varepsilon_n a_n^\dagger a_n, & \hat{P}_{-,n} &= \delta_n \hat{I} + \varepsilon_n a_n a_n^\dagger, \\ \delta_n &= \frac{1}{2} (\sqrt{2 - \varepsilon_n^2} - \varepsilon_n), & 0 &\leq \varepsilon_n \leq 1. \end{aligned} \quad (2.2)$$

The operators  $a_n, a_n^\dagger$  are Majorana fermion operators at  $E > 0$ , with anticommutation relations [23]

$$\{a_n^\dagger, a_m\} = \delta_{nm}, \quad \{a_n, a_m\} = 0. \quad (2.3)$$

The coefficients  $\varepsilon_n, \delta_n$  are chosen such that

$$\hat{P}_{+,n}^2 + \hat{P}_{-,n}^2 = \hat{I}. \quad (2.4)$$

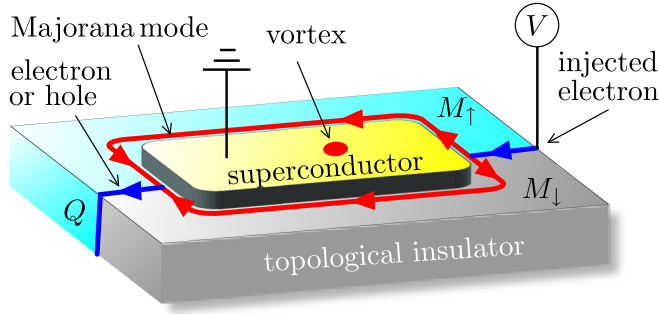


FIG. 1. Layout of the  $\mathbb{Z}_2$  interferometer [3,4]. A three-dimensional topological insulator is covered by magnetic insulators with opposite polarization ( $M_\downarrow$  and  $M_\uparrow$ ) and by a superconductor. A pair of chiral Majorana modes flow along the edge between superconductor and magnet. A bias voltage  $V$  injects an electron into a superposition of the two Majorana modes, which then recombine either as an electron or as a hole after having encircled a certain number of  $h/2e$  vortices. The transferred charge  $Q$  depends on the  $\mathbb{Z}_2$ -valued parity of the number of vortices.

The which-path measurement (2.2) is preceded and followed by unitary propagation, with scattering operators  $\hat{S}_{\text{in}}$  and  $\hat{S}_{\text{out}}$ .

The incoming modes are in thermal equilibrium at inverse temperature  $\beta$ . The corresponding density matrix  $\hat{\rho}_{\text{in}}$  is an operator in Fock space given by

$$\hat{\rho}_{\text{in}} = Z^{-1} e^{-\beta a^\dagger H a}, \quad Z = \text{Tr} e^{-\beta a^\dagger H a}. \quad (2.5)$$

We have collected the operators  $a_n, a_n^\dagger$  in vectors  $a, a^\dagger$ , so that  $a^\dagger H a = \sum_{n,m} a_n^\dagger H_{nm} a_m$ . The single-particle Hamiltonian is [3,4]

$$H = \Omega \begin{pmatrix} H_0(\mathbf{M}) & \Delta \\ \Delta^* & -H_0(-\mathbf{M}) \end{pmatrix} \Omega^\dagger, \quad \Omega = \frac{1}{\sqrt{2}} \begin{pmatrix} 1 & 1 \\ i & -i \end{pmatrix},$$

$$H_0(\mathbf{M}) = \mathbf{M} \cdot \boldsymbol{\sigma} + v_F \mathbf{p} \cdot \boldsymbol{\sigma} - E_F, \quad (2.6)$$

where the unitary matrix  $\Omega$  transforms from the electron-hole basis to the Majorana basis.

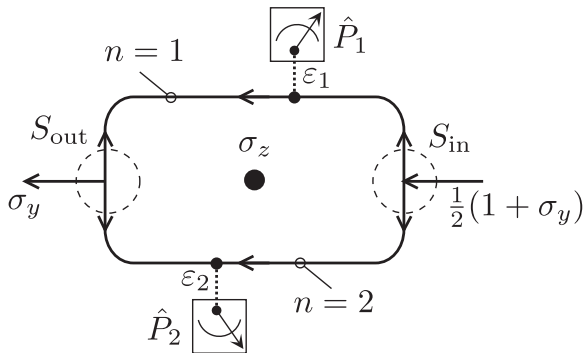


FIG. 2. Scattering geometry corresponding to Fig. 1. The operators  $\hat{P}_1$  and  $\hat{P}_2$  are weak measurements of the occupation number of chiral Majorana modes  $n = 1, 2$ . The vortex (black dot) inserts a  $\pi$  phase shift between the two modes (Pauli matrix  $\sigma_z$ ). At the entrance the matrix  $(1 + \sigma_y)/2$  projects onto an incoming electron, at the exit the matrix  $\sigma_y$  measures the transferred charge. All of this is in the Majorana basis, in the electron-hole basis the role of  $\sigma_y$  and  $\sigma_z$  is interchanged.

The outgoing modes have the density matrix of a monitored quantum channel [13],

$$\hat{\rho}_{\text{out}} = \sum_{s_1, s_2 = \pm} \hat{\mathcal{K}}_{s_1, s_2} \hat{\rho}_{\text{in}} \hat{\mathcal{K}}_{s_1, s_2}^\dagger, \quad (2.7)$$

$$\hat{\mathcal{K}}_{s_1, s_2} = \hat{S}_{\text{out}} \hat{P}_{s_1, 1} \hat{P}_{s_2, 2} \hat{S}_{\text{in}}.$$

The Kraus operators  $\hat{\mathcal{K}}_\pm$  satisfy the sum rule

$$\sum_{s_1, s_2 = \pm} \hat{\mathcal{K}}_{s_1, s_2}^\dagger \hat{\mathcal{K}}_{s_1, s_2} = \hat{I}, \quad (2.8)$$

in view of Eq. (2.4) and the unitarity of  $\hat{S}$ . This ensures that  $\text{Tr} \hat{\rho}_{\text{out}} = \text{Tr} \hat{\rho}_{\text{in}} = 1$ ; the quantum channel (2.7) is a completely positive trace-preserving map [14].

The elastic scattering operator  $\hat{S}$  at energy  $E$  is the exponent of a quadratic form in the fermionic operators,

$$\hat{S} = e^{ia^\dagger L(E) a}, \quad (2.9)$$

with  $L(E)$  a Hermitian  $2 \times 2$  matrix. The unitary matrix  $S(E) = e^{iL(E)}$  is the single-particle scattering matrix. The two scattering operators  $\hat{S}_{\text{in}}$  and  $\hat{S}_{\text{out}}$  are thus represented by a pair of unitary  $2 \times 2$  matrices  $S_{\text{in}}$  and  $S_{\text{out}}$ .

The charge operator  $\hat{Q}$  in the Majorana basis is

$$\hat{Q} = i(a_2^\dagger a_1 - a_1^\dagger a_2) = a^\dagger \sigma_y a. \quad (2.10)$$

(The Pauli matrix  $\sigma_y$  would be  $\sigma_z$  in the electron-hole basis.) The moment generating function  $F(\xi, E)$  of the transferred charge at energy  $E$  is given by

$$F(\xi, E) = \text{Tr} \hat{\rho}_{\text{out}} e^{\xi \hat{Q}} = Z^{-1} \sum_{s_1, s_2 = \pm} \hat{\mathcal{K}}_{s_1, s_2} e^{-\beta a^\dagger H a} \hat{\mathcal{K}}_{s_1, s_2}^\dagger e^{\xi a^\dagger \sigma_y a}. \quad (2.11)$$

At this stage it is helpful to assume  $\varepsilon_n \neq 1$ . (We can later reach  $\varepsilon_n = 1$  by taking the limit.) For  $0 \leq \varepsilon_n < 1$  the projectors  $\hat{P}_{\pm, n}$  have a Gaussian representation [13],

$$\hat{P}_{\pm, n} = c_{\pm, n} e^{\pm \gamma_n a_n^\dagger a_n}, \quad \gamma_n = \ln(1 + \varepsilon_n / \delta_n), \quad (2.12)$$

$$c_{+, n} = \delta_n, \quad c_{-, n} = \varepsilon_n + \delta_n.$$

Traces of products of Gaussian operators can be evaluated by means of Klich's trace-determinant relation [24],

$$\text{Tr} e^{a^\dagger A_1 a} e^{a^\dagger A_2 a} \dots e^{a^\dagger A_p a} = \text{Det}(1 + e^{A_1} e^{A_2} \dots e^{A_p}), \quad (2.13)$$

$$\Rightarrow F(\xi, E) = \sum_{s_1, s_2 = \pm} c_{s_1}^2 c_{s_2}^2 \text{Det}(1 + e^{-\beta H})^{-1} \times \text{Det}(1 + \mathcal{S}_{s_1, s_2} e^{-\beta H} \mathcal{S}_{s_1, s_2}^\dagger e^{\xi \sigma_y}) = \sum_{s_1, s_2 = \pm} c_{s_1}^2 c_{s_2}^2 \text{Det}(1 + \mathcal{N}_{\text{in}}[\mathcal{S}_{s_1, s_2}^\dagger e^{\xi \sigma_y} \mathcal{S}_{s_1, s_2} - 1]). \quad (2.14)$$

We have defined

$$\mathcal{S}_{s_1, s_2} = S_{\text{out}} e^{s_1 \gamma_1 |1\rangle\langle 1|} e^{s_2 \gamma_2 |2\rangle\langle 2|} S_{\text{in}}, \quad (2.15)$$

$$\mathcal{N}_{\text{in}} = (1 + e^{\beta H})^{-1}.$$

The operators  $|1\rangle\langle 1|$  and  $|2\rangle\langle 2|$  project, respectively, on the mode in the upper and lower arm of the interferometer.

In the zero-temperature limit, and for positive bias voltage, only electrons are injected, so that  $\mathcal{N}_{\text{in}}$  is a projector,

$$\mathcal{N}_{\text{in}} = \Omega \begin{pmatrix} 1 & 0 \\ 0 & 0 \end{pmatrix} \Omega^\dagger = \frac{1}{2}(1 + \sigma_y), \quad (2.16)$$

within the energy range  $0 < E < eV$ . Equation (2.14) generalizes the Levitov-Lesovik formula for full counting statistics [15,16], to include the effects of weak measurements [13].

*Binomial charge transfer statistics.* The key difference between the quantum Hall interferometer studied in Ref. [13] and the Majorana interferometer considered here is the constraint of particle-hole symmetry, which requires that

$$S(-E) = S^*(E). \quad (3.1)$$

Both  $S_{\text{in}}$  and  $S_{\text{out}}$  contain contributions from the junction where the two Majorana modes combine into a Dirac mode (an electron-hole mode). We represent each junction by a point scatterer, of dimension small compared to  $\hbar v_F/eV$ , with  $v_F$  the Fermi velocity. The scattering matrix of the junction may then be evaluated at the Fermi level,  $E = 0$ , when it is an element  $e^{i\alpha\sigma_y}$  of  $\text{SO}(2)$ .

Propagation along the interferometer does not couple the Majorana modes, the relative phase shift at energy  $E$  is  $e^{ik\delta L\sigma_z}$ , with  $k = \frac{1}{2}E/\hbar v_F$  and  $\delta L = L_1 - L_2$  the path length difference along the two arms. Each  $h/2e$  vortex in addition contributes a  $\pi$  relative phase shift, so a factor  $\sigma_z^{N_v}$  for  $N_v$  vortices. All together we have

$$\begin{aligned} S_{\text{in}} &= \sigma_z^{N_v} e^{ik\delta L\sigma_z} e^{i\alpha_{\text{in}}\sigma_y}, \\ S_{\text{out}} &= e^{i\alpha_{\text{out}}\sigma_y}. \end{aligned} \quad (3.2)$$

Since the phase shifts  $\propto \sigma_z$  commute with the projective measurements, we may associate them either with  $S_{\text{in}}$  or  $S_{\text{out}}$ —their order relative to the measurements does not matter.

Evaluation of the determinant (2.14) gives the result

$$F(\xi, E) = \cosh \xi + s_v(1 - p_1)(1 - p_2) \cos(2k\delta L) \sinh \xi, \quad (3.3)$$

where  $s_v = (-1)^{N_v}$  is the vortex parity and  $p_n = \varepsilon_n^2$  is the probability of which-path detection in mode  $n$ . Notice that the dependence on  $p_2$  drops out once  $p_1 = 1$ , which is as it should be: since the injected electron passes through the interferometer either in Majorana mode 1 or in Majorana mode 2, once the occupation of mode 1 is measured, it no longer matters whether the occupation of mode 2 is measured or not.

A final simplification applies at low voltages  $V \ll \hbar v_F/e\delta L$ . We can then replace  $\cos(2k\delta L) \approx 1$  in the energy range  $0 < E < eV$ , and the cumulant generating function takes the form

$$\begin{aligned} C(\xi) &= N_{\text{in}} \ln[\cosh \xi + s_v(1 - p_1)(1 - p_2) \sinh \xi], \\ &= N_{\text{in}}(s_v \xi + \ln[1 - \mathcal{T} + \mathcal{T}e^{-2s_v\xi}]), \end{aligned} \quad (3.4a)$$

$$\mathcal{T} = \frac{1}{2}(p_1 + p_2 - p_1 p_2). \quad (3.4b)$$

The number

$$N_{\text{in}} = eV/\delta E = eV t_{\text{counting}}/h \quad (3.5)$$

is the number of electrons injected in the interferometer during the counting time  $t_{\text{counting}}$ , in the large-time limit when the discreteness of  $N_{\text{in}}$  can be ignored [25].

Equation (3.4) combines a deterministic transfer of  $s_v$  electron charges and a stochastic transfer of  $-2s_v$  charges with probability  $\mathcal{T} \in (0, 1/2)$ . The corresponding probability distribution function of the transferred charge  $Q$  is binomial,

$$P(Q) = \binom{N_{\text{in}}}{\frac{1}{2}(N_{\text{in}} - s_v Q)} \mathcal{T}^{\frac{1}{2}(N_{\text{in}} - s_v Q)} (1 - \mathcal{T})^{\frac{1}{2}(N_{\text{in}} + s_v Q)}, \quad (3.6a)$$

$$Q \in \{-N_{\text{in}}, -N_{\text{in}} + 2, \dots, N_{\text{in}} - 2, N_{\text{in}}\}. \quad (3.6b)$$

In the full detection limit  $p_1 \rightarrow 1$  or  $p_2 \rightarrow 1$ , when  $\mathcal{T} \rightarrow 1/2$ , this becomes independent of the vortex number parity  $s_v$ ,

$$P(Q) = 2^{-N_{\text{in}}} \binom{N_{\text{in}}}{\frac{1}{2}(N_{\text{in}} - Q)}, \quad \text{if } \mathcal{T} = \frac{1}{2}. \quad (3.7)$$

The mean and variance of the transferred charge are

$$\bar{Q} = s_v N_{\text{in}}(1 - 2\mathcal{T}) = s_v N_{\text{in}}(1 - p_1)(1 - p_2), \quad (3.8)$$

$$\text{Var } Q = 4N_{\text{in}}\mathcal{T}(1 - \mathcal{T}) = N_{\text{in}}[1 - (1 - p_1)^2(1 - p_2)^2]. \quad (3.9)$$

In a transport measurement one can access these as the electrical conductance and shot noise power [17]. Their dimensionless ratio, the Fano factor

$$F = \frac{\text{Var } Q}{|\bar{Q}|} = \frac{\mathcal{T}(1 - \mathcal{T})}{1 - 2\mathcal{T}}, \quad (3.10)$$

diverges in the limit  $\mathcal{T} \rightarrow 1/2$  of a fully projective measurement (see Fig. 3).

The divergence appears because the projection forces the charge to be transferred via an unpaired Majorana mode. This mode is charge neutral on average but not in an eigenstate of charge, so  $\bar{Q} = 0$  while  $\text{Var } Q \neq 0$  [26]. Because the charge neutrality of the unpaired Majorana mode is not restricted to the Fermi energy, we expect the divergence of the Fano factor to persist at finite temperatures, when an energy range  $k_B T$  around  $E_F$  contributes.

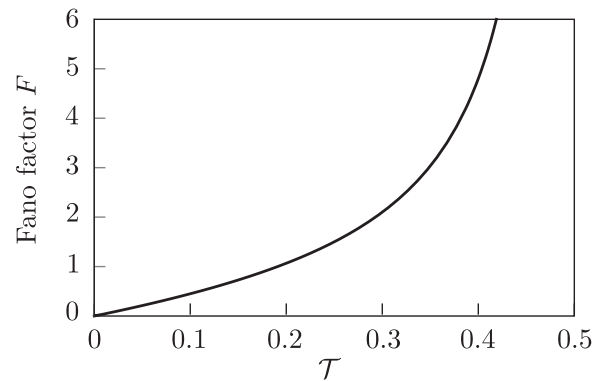


FIG. 3. Fano factor as a function of  $\mathcal{T} = \frac{1}{2}(p_1 + p_2 - p_1 p_2)$ , computed from Eq. (3.10). This dimensionless ratio of shot noise power and conductance increases without bounds as the which-path detection probability tends towards unity (as  $\mathcal{T} \rightarrow 1/2$ ).

*Conclusion.* In summary, we have investigated the effect on the  $\mathbb{Z}_2$  interferometer [3,4] of a weak measurement, capable of partially or fully distinguishing whether a Majorana fermion propagates through the upper or lower arm of the interferometer. Such a measurement fundamentally alters the interference by introducing which-path information, thereby degrading the coherence between the two paths.

We find that a which-path measurement adds a stochastic contribution with binomial statistics to the deterministic charge transfer. This contribution is measurable as a shot noise of the electrical current passed through the interferometer in response to a bias voltage. We note that shot noise of an unpaired Majorana mode is known to have a trinomial statistics [9,27], distinct from the binomial form found here.

We obtained simple expressions for the full counting statistics, dependent only on the probability of the which-path

detection, by working with a high-level description of the measurement as a Gaussian quantum channel [13]. In the present context one source of which-path information is provided by the charge fluctuations of a chiral Majorana mode, coupled to the electromagnetic environment. One would need a microscopic model of this coupling [28], to find out how effective the which-path measurement is in a realistic geometry. We hope that the striking effect of the coupling presented here, a divergent Fano factor, will motivate such a modeling.

*Acknowledgments.* This work was supported by the Netherlands Organisation for Scientific Research (NWO/OCW), as part of Quantum Limits (Project No. SUMMIT.1.1016). I have benefited from discussions with A. R. Akhmerov and F. Hassler.

*Data availability.* No data were created or analyzed in this study.

- 
- [1] A. Altland and M. R. Zirnbauer, Nonstandard symmetry classes in mesoscopic normal-superconducting hybrid structures, *Phys. Rev. B* **55**, 1142 (1997).
- [2] C. W. J. Beenakker and L. P. Kouwenhoven, A road to reality with topological superconductors, *Nature Phys.* **12**, 618 (2016).
- [3] L. Fu and C. L. Kane, Probing neutral Majorana fermion edge modes with charge transport, *Phys. Rev. Lett.* **102**, 216403 (2009).
- [4] A. R. Akhmerov, J. Nilsson, and C. W. J. Beenakker, Electrically detected interferometry of Majorana fermions in a topological insulator, *Phys. Rev. Lett.* **102**, 216404 (2009).
- [5] K. T. Law, P. A. Lee, and T. K. Ng, Majorana fermion induced resonant Andreev reflection *Phys. Rev. Lett.* **103**, 237001 (2009).
- [6] G. Strübi, W. Belzig, M. S. Choi, and C. Bruder, Interferometric and noise signatures of Majorana fermion edge states in transport experiments, *Phys. Rev. Lett.* **107**, 136403 (2011).
- [7] J. Li, G. Fleury, and M. Büttiker, Scattering theory of chiral Majorana fermion interferometry, *Phys. Rev. B* **85**, 125440 (2012).
- [8] S. Park, J. E. Moore, and H.-S. Sim, Absence of Aharonov-Bohm effect of chiral Majorana fermion edge states, *Phys. Rev. B* **89**, 161408(R) (2014).
- [9] G. Strübi, W. Belzig, T. L. Schmidt, and C. Bruder, Full counting statistics of Majorana interferometers, *Physica E* **74**, 489 (2015).
- [10] D. S. Shapiro, A. D. Mirlin, and A. Shnirman, Microwave response of a chiral Majorana interferometer, *Phys. Rev. B* **104**, 035434 (2021).
- [11] E. Buks, R. Schuster, M. Heiblum, D. Mahalu, and V. Umansky, Dephasing in electron interference by a 'which-path' detector, *Nature (London)* **391**, 871 (1998).
- [12] D. Sprinzak, E. Buks, M. Heiblum, and H. Shtrikman, Controlled dephasing of electrons via a phase sensitive detector, *Phys. Rev. Lett.* **84**, 5820 (2000).
- [13] C. W. J. Beenakker and J.-F. Chen, Monitored quantum transport: Full counting statistics of a quantum Hall interferometer, [arXiv:2504.07773](https://arxiv.org/abs/2504.07773).
- [14] M. A. Nielsen and I. L. Chuang, *Quantum Computation and Quantum Information* (Cambridge University Press, Cambridge, 2010).
- [15] L. S. Levitov and G. B. Lesovik, Charge distribution in quantum shot noise, *JETP Lett.* **58**, 230 (1993).
- [16] L. S. Levitov, H.-W. Lee and G. B. Lesovik, Electron counting statistics and coherent states of electric current, *J. Math. Phys.* **37**, 4845 (1996).
- [17] Ya. M. Blanter and M. Büttiker, Shot noise in mesoscopic conductors, *Phys. Rep.* **336**, 1 (2000).
- [18] F. Marquardt and C. Bruder, Influence of dephasing on shot noise in an electronic Mach-Zehnder interferometer, *Phys. Rev. Lett.* **92**, 056805 (2004); Effects of dephasing on shot noise in an electronic Mach-Zehnder interferometer, *Phys. Rev. B* **70**, 125305 (2004).
- [19] V. S.-W. Chung, P. Samuelsson, and M. Büttiker, Visibility of current and shot noise in electrical Mach-Zehnder and Hanbury Brown Twiss interferometers, *Phys. Rev. B* **72**, 125320 (2005).
- [20] S. Pilgram, P. Samuelsson, H. Förster, and M. Büttiker, Full-counting statistics for voltage and dephasing probes, *Phys. Rev. Lett.* **97**, 066801 (2006).
- [21] H. Förster, P. Samuelsson, S. Pilgram, and M. Büttiker, Voltage and dephasing probes in mesoscopic conductors: A study of full-counting statistics, *Phys. Rev. B* **75**, 035340 (2007).
- [22] A. Helzel, L. V. Litvin, I. P. Levkivskyi, E. V. Sukhorukov, W. Wegscheider, and C. Strunk, Counting statistics and dephasing transition in an electronic Mach-Zehnder interferometer, *Phys. Rev. B* **91**, 245419 (2015).
- [23] Without the restriction to positive energies the anticommutator (2.3) of two annihilation operators does not vanish, because of the particle-hole symmetry relation  $a(E) = a^\dagger(-E)$ . This plays a role when inelastic scattering couples positive and negative energies, see, C. W. J. Beenakker, Annihilation of colliding Bogoliubov quasiparticles reveals their Majorana nature, *Phys. Rev. Lett.* **112**, 070604 (2014).
- [24] I. Klich, An elementary derivation of Levitov's formula, in *Quantum Noise in Mesoscopic Physics*, NATO Science Series II (Kluwer Academic Publishers, Dordrecht, The Netherlands, 2003), Vol. 97, p. 397.
- [25] F. Hassler, M. V. Suslov, G. M. Graf, M. V. Lebedev, G. B. Lesovik, and G. Blatter, Wave-packet formalism of full counting statistics, *Phys. Rev. B* **78**, 165330 (2008). Finite detection-time corrections have been considered in this

- Letter, they modify the binomial statistics with terms of order  $N_{\text{in}}^{-1} \ln N_{\text{in}}$ ,  $N_{\text{in}} = eVt_{\text{counting}}/h$ .
- [26] A. R. Akhmerov, J. P. Dahlhaus, F. Hassler, M. Wimmer, and C. W. J. Beenakker, Quantized conductance at the Majorana phase transition in a disordered superconducting wire, *Phys. Rev. Lett.* **106**, 057001 (2011).
- [27] N. V. Gnedilov, B. van Heck, M. Diez, J. A. Hutasoit, and C. W. J. Beenakker, Topologically protected charge transfer along the edge of a chiral p-wave superconductor, *Phys. Rev. B* **92**, 121406(R) (2015).
- [28] C. Knapp, T. Karzig, R. M. Lutchyn, and C. Nayak, Dephasing of Majorana-based qubits, *Phys. Rev. B* **97**, 125404 (2018).